

## Dimerization Region of Soluble Guanylate Cyclase Characterized by Bimolecular Fluorescence Complementation *in vivo*

Christiane Rothkegel, Peter M. Schmidt, Derek-John Atkins, Linda Sarah Hoffmann, Harald H.H.W Schmidt, Henning Schröder, and Johannes-Peter Stasch

*Cardiovascular Research, Bayer HealthCare, Aprather Weg 18a, D-42096 Wuppertal, Germany (C.R., D.J.A., L.S.H., J.P.S.), Martin-Luther-University, School of Pharmacy, Wolfgang-Langenbeck-Strasse 4, D-06120 Halle, Germany (C.R., L.S.H., H.S., J.P.S.), Department of Pharmacology, Monash University, Melbourne, Clayton, VIC 3800, Australia (P.M.S., H.H.H.W.S.), Department of Pharmaceutics, College of Pharmacy, University of Minnesota, Minneapolis, MN 55455, USA (H.S.), and Helios Klinikum, Institute for Pathology, Heusnerstrasse 40, D-42283 Wuppertal, Germany (D.J.A)*

**Running Title:** Dimerization of soluble guanylate cyclase

**Corresponding author**

Priv.-Doz. Dr. Johannes-Peter Stasch

Bayer HealthCare

Cardiovascular Research

Aprather Weg 18a

D-42096 Wuppertal

Germany

Phone: +49-202-368738

Fax: +49-202-368009

E-Mail: johannes-peter.stasch@bayerhealthcare.com

**Document statistics**

Number of text pages: 24

Number of tables: 2

Number of figures: 6

Number of references: 42

Number of words in the *Abstract*: 160

Number of words in the *Introduction*: 550

Number of words in the *Discussion*: 1650

**Abbreviations list**

Abbreviations used in this paper: BiFC, bimolecular fluorescence complementation; CBS, C-terminal binding site; cGMP, cyclic GMP; sGC, soluble guanylate cyclase; NBS, N-terminal binding site; NO, nitric oxide; WT, wildtype; YC, C-terminal fragment of YFP; YN, N-terminal fragment of YFP.

## Abstract

The ubiquitously expressed nitric oxide (NO) receptor soluble guanylate cyclase (sGC) plays a key role in signal transduction. Binding of NO to the N-terminal prosthetic heme moiety of sGC results in an approximate 200-fold activation of the enzyme and an increased conversion of GTP into the second messenger cyclic GMP (cGMP). sGC exists as a heterodimer whose dimerization is mediated mainly by the central region of the enzyme. In the present work, we constructed deletion mutants within the predicted dimerization region of the sGC  $\alpha_1$ - and  $\beta_1$ -subunit to precisely map the sequence segments crucial for subunit dimerization. To track mutation-induced alterations of sGC dimerization we used a bimolecular fluorescence complementation (BiFC) approach which allows visualizing sGC heterodimerization in a non-invasive manner in living cells. Our study suggests that segments spanning amino acids  $\alpha_1$ 363-372,  $\alpha_1$ 403-422,  $\alpha_1$ 440-459 and  $\beta_1$ 212-222,  $\beta_1$ 304-333,  $\beta_1$ 344-363,  $\beta_1$ 381-400 within the predicted dimerization region are involved in the process of heterodimerization and therefore in the expression of functional sGC.

## Introduction

sGC is the ubiquitously expressed intracellular receptor for the gaseous biological messenger NO. The enzyme is activated upon binding of its endogenous activator NO to its heme moiety, resulting in a strongly increased conversion of GTP to cGMP. This second messenger regulates various effector systems such as phosphodiesterases, ion channels and protein kinases. Thus, the NO/sGC/cGMP pathway modulates a broad range of physiological processes including vasodilatation, neurotransmission and platelet aggregation (Hobbs, 2002; Bender and Beavo, 2006; Feil and Kemp-Harper, 2006). Due to its ubiquitous nature, the pathogenesis of various disease states, especially of the cardiovascular system, has been linked to aberrant activation of the NO/sGC/cGMP pathway (Hobbs, 2002; Feil and Kemp-Harper, 2006; Gladwin, 2006; Stasch et al., 2006)

sGC is a heterodimer consisting of an  $\alpha$ - and a heme-containing  $\beta$ -subunit. Although two isoforms of each subunit ( $\alpha_1$ ,  $\alpha_2$ ,  $\beta_1$  and  $\beta_2$ ) exist, only the ubiquitous expressed  $\alpha_1/\beta_1$ -heterodimer and the  $\alpha_2/\beta_1$ -heterodimer, which is most abundant in brain, uterus and placenta, have been characterized as functional enzymes (Harteneck et al., 1991; Russwurm et al., 1998; Zabel et al., 1998; Hönicka et al., 1999; Mergia et al., 2003). Since the crystal structure of sGC has not been resolved yet, most of the knowledge of the enzyme's spatial structure is based on homology to other crystallized proteins, in silico structure predictions, and biochemical approaches such as mutagenesis, enzymatic assays, or co-immunoprecipitations. Based on these results the sGC subunits have been divided into distinct regions: the N-terminal NO sensing heme domain (H-NOX), the central region consisting of a PAS-like domain and an amphipathic  $\alpha$ -helix region, and the C-terminal highly conserved catalytic domain (Gerzer et al., 1981; Nioche et al., 2004; Pellicena et al., 2004; Cary et al., 2006). The  $\beta$  H-NOX domain contains the prosthetic heme group which is coordinated to this domain via the axial ligand His<sub>105</sub>, and the recently identified heme-binding motif Tyr<sub>135</sub>, Ser<sub>137</sub> and Arg<sub>139</sub> (Y-x-S-x-R) (Wedel et al., 1994; Zhao et al., 1998; Pellicena et al., 2004; Schmidt et al., 2004; 2005). Dimerization of the  $\alpha/\beta$ -subunits has been proposed to be mediated mainly by the central region of sGC based on the homology of amino acids  $\beta_1$ 340-385 to the sequence mediating particulate guanylate cyclase homodimerization and studies that identified segments spanning amino acids  $\alpha_1$ 61-128,  $\alpha_1$ 367-462,  $\alpha_1$ 421-454,  $\beta_1$ 204-244, and  $\beta_1$ 379-408 to be responsible for subunit dimerization (Wilson and Chinkers, 1995; Zhao and Marletta, 1997; Nighorn et al., 1999; Zhou et al., 2004; Shiga and Suzuki, 2005; Wagner et al., 2005).

To further narrow the published and to identify novel amino acid segments involved in sGC heterodimerization, we identified conserved parts of the central domain of sGC via multi



sequence alignments and systematically deleted these residues. The impact of these alterations on the formation of functional sGC was determined by BiFC which enabled us to visualize sGC heterodimerization in a non-invasive manner in living cells. In parallel we investigated the activation profile of the generated mutants by using a unique cGMP reporter cell line. This cell line in combination with NO- and heme-independent sGC activators, such as BAY 58-2667, and NO-independent but heme-dependent sGC stimulators, such as BAY 41-2272, enabled us to characterize the activation profile of sGC and sGC variants directly within their cellular environment (Stasch et al., 2001; Schmidt et al., 2005; Wunder et al., 2005; Rothkegel et al., 2006).

## Materials and Methods

### Reagents

BAY 58-2667 (4-[[[(4-carboxybutyl){2-[(4-phenethyl-benzyl)oxy]-phenethyl}amino)methyl[benzoic]acid) and BAY 41-2272 (5-cyclopropyl-2-[1-(2-fluoro-benzyl)-1H-pyrazolo[3,4-b]pyridin-3-yl]-pyrimidin-4-ylamine) were synthesized as described (Alonso-Alija et al., 2001; Straub et al., 2001). DEA/NO (2-(N,N-diethylamino)-diazene-2-oxide) and ODQ (1H-(1,2,4)-oxadiazole-(4,3-a)-quinoxalin-1-one) were purchased from Alexis Biochemicals (San Diego, USA). All other chemicals of analytical grade were obtained from Sigma (Taufkirchen, Germany).

### Construction of fusion proteins for BiFC analysis

The plasmids pBiFC-YN154 and pBiFC-YC155 were kindly provided by Dr. T. Kerppola (University of Michigan, Ann Arbor, USA) and encoded amino acids 1 to 154 (YN) and 155 to 238 (YC) of enhanced YFP (Hu et al., 2002). The sequences encoding YN and YC are preceded by the linker sequences RPACKIPNDLKQKVMNH and RSIAT, respectively. To construct proteins fused to either the N-terminus (YNV, YCV) or the C terminus (YNH, YCH) of sGC, sequences encoding the rat  $\alpha_1$ - or the  $\beta_1$ -subunit were cloned into pBiFC-YN154 and pBiFC-YC155. Sequences encoding  $\alpha_1$ -sGC and  $\beta_1$ -sGC were amplified by PCR from pcDNA/Amp and pRNAI/Amp. Primers listed in Table I introduced a BsiWI site and a ClaI site in pcDNA/Amp, pRNAI/Amp, pBiFC-YN154 and pBiFC-YC155. The  $\alpha_1$ -sGC and  $\beta_1$ -sGC PCR products were digested with BsiWI and ClaI (Roche, Basel) and inserted into the pBiFC-YN154 and pBiFC-YC155 plasmids digested with the same enzymes, to produce the N-terminal fused chimeras  $\alpha_1$ -YNV,  $\alpha_1$ -YCV,  $\beta_1$ -YNV,  $\beta_1$ -YCV and the C-terminal fused chimeras  $\alpha_1$ -YNH,  $\alpha_1$ -YCH,  $\beta_1$ -YNH,  $\beta_1$ -YCH respectively. The integrity of all clones was verified by sequence analysis (Invitex, Berlin, Germany).

### Cell culture and transient transfection

The transient cotransfection of  $\alpha_1$ - and  $\beta_1$ -subunits was based on a method recently described (Schmidt et al., 2005; Rothkegel et al., 2006). Briefly, for cGMP readout, cGMP reporter cells were seeded on 96-well microtiter plates at a density of 10,000 cells per well. For confocal microscopy, cGMP reporter cells were seeded in 8-well glass chambers (NuncNalgene, Naperville, USA) at a density of 20,000 cells per chamber. Cells were cultured for 1 day at 37°C, 5% CO<sub>2</sub> and then cotransfected with a transfection mixture containing 36 ng  $\alpha_1$ - and 36 ng  $\beta_1$ -plasmid, 0.12  $\mu$ l Plus<sup>®</sup> reagent and 0.6  $\mu$ l of LipofectAMINE<sup>®</sup> (Invitrogen, Carlsbad, USA) in 100  $\mu$ l Opti-MEM<sup>®</sup> serum-free medium (Invitrogen) or 250 ng  $\alpha_1$ - and 250 ng  $\beta_1$ -plasmid, 0.84  $\mu$ l

Plus<sup>®</sup> reagent and 4.2  $\mu$ l of LipofectAMINE<sup>®</sup> (Invitrogen) in 200  $\mu$ l Opti-MEM<sup>®</sup> serum-free medium, respectively. After 3 h the serum-free medium was exchanged by serum-containing medium and cells were incubated for 24 h at 37°C, 5% CO<sub>2</sub> to ensure optimal protein expression.

### **cGMP readout**

The generation of the cGMP reporter cell and the cGMP readout has been previously described (Schmidt et al., 2005; Wunder et al., 2005; Rothkegel et al., 2006). Briefly, for the determination of the sGC activation profile, transiently transfected cGMP reporter cells were incubated with various concentrations of the sGC stimulator, BAY 41-2272 or sGC activator, BAY 58-2667 alone or in presence of DEA/NO or ODC for 15 min at 37°C, 5% CO<sub>2</sub>. 3-Isobutyl-1-methylxanthin (IBMX, 0.2 mM) was used to prevent cGMP degradation by endogenous phosphodiesterases. The bioluminescence readout was initiated by application of 10 mM CaCl<sub>2</sub> containing buffer and was shown to correlate directly with the intracellular cGMP concentration as described elsewhere (Wunder et al., 2005).

### **BiFC analysis by confocal microscopy**

For analysis of individual cells by confocal microscopy, the transiently transfected cGMP reporter cells grown in 8-well glass chambers were examined with a Zeiss Confocal Microscope LSM 510 (Carl Zeiss, Jena, Germany) using an oilplan 63 x objective (Carl Zeiss, Jena, Germany). YFP was excited at 514 nm and detected at 530 to 600 nm. Images were taken with an integrated CCD-camera, processed and analyzed with the LSM Image software (Carl Zeiss, Jena, Germany). To adjust size and contrast the images were further processed with Photoshop software (Adobe, München, Germany).

### **Western blotting**

To validate the transient expression of sGC in the cGMP reporter cell line, cells were transfected as described above. After 24 h, cells were lysed and centrifuged at 100,000 x g. Proteins of the supernatant (10  $\mu$ g) were separated on a 10% polyacrylamide gel (Anamed, Darmstadt, Germany) by electrophoresis as previously described (Rothkegel et al., 2006). The protein bands were transferred to a nitrocellulose membrane (Mini-PROTEAN<sup>®</sup> II cell, Trans-Blot Transfer Medium Pure Nitrocellulose Membran<sup>®</sup>, 0.2  $\mu$ M, Bio-Rad, Munich, Germany). The individual sGC subunits were detected using polyclonal antibodies directed against epitopes of the  $\alpha_1$ -sGC and the  $\beta_1$ -sGC subunits (Cayman, Tallin, Estonia). Actin was used as a loading

control and detected by a monoclonal anti- $\beta$ -actin antibody (Sigma, Taufkirchen, Germany). Detection was performed by ECL method (Becker et al., 1999).

### **Mutagenesis**

The mutagenesis was performed using the QuickChange-XL<sup>®</sup> site-directed mutagenesis kit (Stratagene, La Jolla, USA) according to manufacturer's instructions. Primers listed in Table II were used to generate the deletion mutants screened by BiFC analysis and in the cGMP readout-system. The accuracy of the mutations was verified by sequencing (Invitex, Berlin, Germany).

## Results

### Generation of functional fluorescent proteins of $\alpha_1/\beta_1$ -sGC

The recently developed BiFC approach was applied to visualize the heterodimerization of  $\alpha_1$ - and  $\beta_1$ -sGC subunits (Hu et al., 2002). In general, this approach is based on the complementation of a fluorophore such as YFP from two non-fluorescent fragments upon interaction of the two proteins fused to each fragment (Kerpolla 2006 a, b).

To construct a fluorescent  $\alpha_1/\beta_1$ -sGC heterodimer we fused the N-terminal YFP fragment (YN) and the C-terminal fragment (YC) to the N-terminus (YNV, YCV) and the C-terminus (YNH, YCH) of the  $\alpha_1$ - and  $\beta_1$ -subunit, respectively (Fig. 1 A). The generated fusion proteins were transiently expressed in a cGMP reporter cell line based on a CHO cell line stably transfected with the cyclic nucleotide gated olfactory CNG2A-channel and cytosolic aequorin (Wunder et al., 2005). Fluorescence was detected by confocal microscopy and enzyme activity was measured as luminescence, indicated in relative light units, which was shown to correlate with the intracellular cGMP concentration (Wunder et al., 2005). Coexpression of  $\alpha_1$ -YCH/ $\beta_1$ -YNH-sGC and  $\alpha_1$ -YNV/ $\beta_1$ -YCV-sGC resulted in a fluorescence signal located in the cytosol (Fig. 1 C and D). Other possible combinations of both complementary YFP fragments did not lead to any detectable fluorescence signal indicating that functional YFP complementation was not achieved (Fig. 1 A). YN-YC-sGC fusion constructs which showed fluorescence complementation were expressed at similar levels (Fig. 1 E). To exclude that the fused YN/YC fragments affect the enzyme's catalytic activity, the activation profile of  $\alpha_1$ -YCH/ $\beta_1$ -YNH-sGC and  $\alpha_1$ -YNV/ $\beta_1$ -YCV-sGC was characterized in the cGMP reporter cell and compared to wildtype (WT)-sGC.

Cotransfection of cGMP reporter cells with WT- $\alpha_1$ - and WT- $\beta_1$ -sGC cDNA resulted in an activation profile characteristic for the native, heme-containing enzyme. The NO-independent, but heme-dependent sGC stimulator BAY 41-2272 stimulated the enzyme in a concentration-dependent manner with an  $EC_{50}$  value of  $467 \pm 13.9$  nM. In the presence of 10 nM DEA/NO which caused a 4.3-fold stimulation, the concentration response curve was shifted to the left reflected by the determined  $EC_{50}$  value of  $205 \pm 12.8$  nM (Fig. 2 A and Fig. 3). The NO- and heme-independent sGC activator BAY 58-2667 induced a 15-fold stimulation ( $EC_{50}$   $69 \pm 9.6$  nM) of enzyme activity, which was further increased up to 30-fold ( $EC_{50}$   $30 \pm 6.6$  nM) in the presence of ODQ (Fig. 2 B). Thus, the activation profile of the cGMP cells transiently transfected with the native enzyme is similar to that observed for isolated sGC.

In contrast to the WT enzyme the  $\alpha_1$ -YCH/ $\beta_1$ -YNH-sGC was unresponsive to BAY 41-2272 or BAY 58-2667 alone or combined with DEA/NO or ODQ, respective, indicating that fusion of the YN/YC-fragments to the sGC catalytic domain disturbed the cGMP-forming capability of the enzyme (Fig. 2 C, D and Fig. 3).

Fusion of the YFP fragments to the N-termini of the  $\alpha$ - and  $\beta$ -subunit of sGC caused only slight alterations of the enzyme's catalytic activity. Coexpression of  $\alpha_1$ -YNN/ $\beta_1$ -YCV-sGC resulted in an activation profile similar to the native, heme-containing enzyme. BAY 41-2272 stimulated the  $\alpha_1$ -YNN/ $\beta_1$ -YCV-sGC concentration dependently with an  $EC_{50}$  value of  $540 \pm 19.5$  nM and addition of 10 nM DEA/NO which stimulates the  $\alpha_1$ -YNN/ $\beta_1$ -YCV-sGC to a maximum of 4.86-fold caused a potentiation of the BAY 41-2272-induced stimulation reducing the  $EC_{50}$  value to  $430 \pm 17.5$  nM (Fig. 2 E and Fig. 3). BAY 58-2667 induced a concentration dependent activation with an  $EC_{50}$  value of  $15 \pm 0.96$  nM which was decreased in the presence of ODQ to  $3.9 \pm 0.66$  nM (Fig. 2 F).

As the C-terminal sGC-BiFC fusion constructs were non-functional, all following experiments were performed with the N-terminal  $\alpha_1$ -YNN/ $\beta_1$ -YCV construct.

### Characterization of the $\alpha_1$ -sGC and $\beta_1$ -sGC deletion mutants

Conserved segments within the predicted dimerization regions of  $\alpha_1$ -sGC and  $\beta_1$ -sGC were identified by a multiple sequence alignment (Fig. 4, red coloured residues). The identified amino acids were deleted and the various constructs were transiently transfected into the cGMP reporter cell for protein expression. The ability of the deletion mutants to heterodimerize was characterized by BiFC and the activation profile was characterized by luminescence as described above.

Coexpression of the  $\alpha_1$ -YNN deletion mutants  $\alpha_1(\Delta 283-292)$ ,  $\alpha_1(\Delta 373-382)$ ,  $\alpha_1(\Delta 383-392)$ ,  $\alpha_1(\Delta 393-402)$ ,  $\alpha_1(\Delta 460-469)$  and  $\alpha_1(\Delta 470-479)$  with WT- $\beta_1$ -YCV as well as the  $\beta_1$ -YCV deletion mutants  $\beta_1(\Delta 334-343)$ ,  $\beta_1(\Delta 401-410)$  and  $\beta_1(\Delta 411-420)$  with WT- $\alpha_1$ -YNN-sGC resulted in a fluorescence signal similar to the fluorophore-tagged WT-enzyme. The observed fluorescence indicates functional heterodimerization of both sGC subunits in the cytosol of the cell (Fig. 5 A).  $\alpha_1(\Delta 393-402)$ ,  $\beta_1(\Delta 334-343)$  and  $\beta_1(\Delta 411-420)$  were mainly localized in focal areas and not in the entire cytosolic department (Fig. 5 A). Coexpression of all other deletion mutants did not result in any detectable fluorescence suggesting a putative involvement of the deleted residues in the process of sGC heterodimerization (Fig. 4, Supplemental data). To exclude that this loss of fluorescence was due to impaired expression or decreased protein stability, expression levels of the transiently transfected deletion mutants were determined by Western blot analysis. As shown in Fig. 5 B all constructs were expressed at a similar level suggesting that the observed lack of fluorescence was due to the inability to form functional sGC  $\alpha_1/\beta_1$ -heterodimers.

Deletion of segments 283-292, 373-382, 383-392, 393-402 of the  $\alpha_1$ -YNN-sGC and 334-343 of  $\beta_1$ -YCV-sGC resulted in the expression of a functionally active enzyme (Fig. 6 A-J). The sGC stimulator BAY 41-2272 stimulated  $\alpha_1(\Delta 283-292)/\beta_1$ -sGC maximal 25-fold. This activation

was potentiated in the presence of DEA/NO up to 150-fold (Fig. 6 A). In the case of  $\alpha_1(\Delta 373-382)/\beta_1$ -sGC BAY 41-2272 induced a concentration dependent enzyme stimulation of maximal 90-fold which was potentiated up to 200-fold upon combination with DEA/NO (Fig. 6 C). The  $\alpha_1(\Delta 383-392)/\beta_1$ -sGC was stimulated by BAY 41-2272 concentration-dependently to a maximum of 3-fold and addition of DEA/NO potentiated the BAY 41-2272 induced enzyme activation up to 10-fold (Fig. 6 E).  $\alpha_1(\Delta 393-402)/\beta_1$ -sGC and  $\alpha_1/\beta_1(\Delta 334-343)$ -sGC were only responsive to a combination of BAY 41-2272 and DEA/NO up to 25-fold and 12-fold, respectively (Fig. 6 G and I). The heme-independent sGC activator BAY 58-2667 induced a concentration dependent activation of  $\alpha_1(\Delta 283-292)/\beta_1$ -sGC to a maximum of 60-fold (Fig. 6 B). The  $\alpha_1(\Delta 373-382)/\beta_1$ -sGC was activated by BAY 58-2667 up to 20-fold and the  $\alpha_1(\Delta 383-392)/\beta_1$ -sGC was activated up to 130-fold (Fig 6 D and F). In the case of  $\alpha_1(\Delta 393-402)/\beta_1$ -sGC and  $\alpha_1/\beta_1(\Delta 334-343)$ -sGC BAY 58-2667 activated the altered enzymes to a maximum of 5-fold and 2-fold, respectively (Fig. 6 H and J). The BAY 58-2667-induced enzyme activation was potentiated in the presence of ODQ for  $\alpha_1(\Delta 373-382)/\beta_1$ -sGC, only (Fig. 6 D). All other deletion mutants were unresponsive to BAY 41-2272, BAY 58-2667 alone or upon combination with DEA/NO or ODQ (see supplemental data).

## Discussion

Protein dimerization frequently leads to changes in ligand affinity, changes in the localization and/or alteration of the enzymatic capacity (Luttrell, 2006). The ubiquitous NO-receptor sGC, which regulates via the conversion of GTP into the second messenger cGMP various effector systems, such as phosphodiesterases, ion channels, and protein kinases, must undergo heterodimerization to obtain catalytic activity (Harteneck et al., 1991; Zabel et al., 1998; Hönicka et al., 1999; Feil and Kemp-Harper, 2006).

The structural basis of sGC heterodimerization is still poorly understood. A decade ago the amino acid region  $\beta_1$ 340-385 upstream the enzyme's catalytic domain was postulated to play a key role in heterodimer formation of sGC. This assumption was based on homologies to the respective sequence mediating dimerization of the membrane bound guanylate cyclase A (GC-A) and supported later on by studies showing that a construct encoding residues 1-385 of  $\beta_1$ -sGC is capable of forming homodimers (Wilson and Chinkers, 1995; Zhao and Marletta, 1997). Subsequent coprecipitation analyses of truncated and/or mutated sGC indicated that segments spanning  $\alpha_1$ 61-128,  $\alpha_1$ 367-462,  $\alpha_1$ 421-454,  $\beta_1$ 204-244 and  $\beta_1$ 379-408 contribute to  $\alpha_1/\beta_1$ -heterodimerization (Zhou et al., 2004; Shiga and Suzuki, 2005; Wagner et al., 2005).

In the present analysis we validated as well as narrowed published sequences and tried to identify novel residues involved in  $\alpha_1/\beta_1$ -sGC heterodimerization. In contrast to published work, we monitored the formation of sGC  $\alpha_1/\beta_1$ -heterodimers and their activation profile in living cells by a unique combination of the BiFC approach and a cGMP reporter cell line (Hu et al., 2002; Schmidt et al., 2004; Wunder et al., 2005; Kerppola 2006 a, b; Rothkegel et al., 2006).

The generally accepted fact that both subunits have developed from a common ancestor and published results showing that sGC  $\alpha$ - and  $\beta$ -subunits are capable of forming homo- as well as heterodimers suggested the existence of a conserved homologous dimerization motif in both subunits of the enzyme (Zhao and Marletta, 1997; Zabel et al., 1999; Iyer et al., 2003). Therefore, we constructed a sequence alignment in order to identify conserved segments within the predicted dimerization regions of  $\alpha_1/\beta_1$ -sGC (Fig. 4). These identified segments were systematically deleted and the generated deletion mutants characterized by transient transfection into the cGMP reporter cell line. The screen of the heterodimerization profile of the deletion mutants by BiFC revealed that coexpression of the deletion mutants  $\alpha_1$ 283-292,  $\alpha_1$ 373-382,  $\alpha_1$ 383-392,  $\alpha_1$ 393-402,  $\alpha_1$ 460-469,  $\alpha_1$ 470-479 with  $\beta_1$ -sGC and  $\beta_1$ 334-343,  $\beta_1$ 401-410 and  $\beta_1$ 411-420 with  $\alpha_1$ -sGC resulted in a fluorescence similar to native  $\alpha_1/\beta_1$ -sGC therefore indicating that these deletion mutants were still able to dimerize and thus the deleted amino acid regions are not involved in  $\alpha_1/\beta_1$ -sGC heterodimerization (Fig. 4; green/yellow shaded



segments). From the above listed deletion mutants which showed fluorescence  $\alpha_1$ 283-292,  $\alpha_1$ 373-382,  $\alpha_1$ 383-392,  $\alpha_1$ 393-402 and  $\beta_1$ 334-343 showed enzymatic activity thus corroborating the results obtained from the BiFC assay. Although some of these deletions ( $\alpha_1$ 283-292,  $\alpha_1$ 373-382,  $\alpha_1$ 393-402 and  $\beta_1$ 334-343) resulted in measurable alterations of the BAY 41-2272 and/or DEA/NO activation profile, the presence of catalytic activity in combination with the observed fluorescence indicated clear-cut the formation of functional heterodimers. These observed alterations of sGC activation as well as the loss of any enzymatic activity in the case of the fluorescent deletion mutants  $\alpha_1$ 460-469,  $\alpha_1$ 470-479,  $\beta_1$ 401-410 and  $\beta_1$ 411-420 suggest that, although these residues might not be critical for sGC dimerization, the mutations directly disturbed or even impaired the mechanism of enzyme activation.

All fluorescent mutants showed a homogenous localization in the cytosol with the exception of the deletion constructs  $\alpha_1$ 393-402,  $\beta_1$ 334-343 and  $\beta_1$ 411-420. Although, Western blot analysis revealed no significant changes in the expression levels of all generated mutants these three deletion mutants showed a more inhomogeneous distribution. This difference might point to deletion-induced problems with regard to proper protein folding that could result in the aggregation of misfolded proteins and, in turn, lead to unspecific BiFC signals (Ozalp et al., 2005). However,  $\alpha_1$ 393-402 and  $\beta_1$ 334-343 were enzymatically active indicating the formation of functional sGC heterodimers. Whether this cGMP formation was catalyzed by potentially aggregated sGC or by a small subpopulation of correctly folded enzyme in the cytosol remains an open question as the cGMP reporter cell does not provide spatial information about the cGMP synthesis as FRET-based methods do (Honda et al., 2001; Nikolaev et al., 2006). Nevertheless, the observed catalytic activity indicates the formation of functional sGC ruling out an involvement of these residues in the process of heterodimerization.

Deletion of amino acid regions  $\alpha_1$ 363-372,  $\alpha_1$ 403-412,  $\alpha_1$ 413-422,  $\alpha_1$ 440-449,  $\alpha_1$ 450-459 and  $\beta_1$ 212-222,  $\beta_1$ 304-313,  $\beta_1$ 314-323,  $\beta_1$ 324-333,  $\beta_1$ 344-353,  $\beta_1$ 354-363,  $\beta_1$ 381-390,  $\beta_1$ 391-400 caused loss of fluorescence and of enzymatic activity. As the corresponding western blots showed unaltered expression levels of the constructed mutant enzymes these results strongly suggest an involvement of these segments in  $\alpha_1/\beta_1$ -sGC heterodimerization (Fig. 4, orange shaded segments)

Regarding the sGC  $\beta_1$ -subunit it has been reported that amino acids  $\beta_1$ 204-408 mediate sGC heterodimerization (Zhou et al., 2004). A more detailed analysis of this region identified two separate contact interfaces of  $\beta_1$ -sGC with  $\alpha_1$ -sGC: an N-terminal binding site (NBS) segment consisting of amino acids  $\beta_1$ 204-244 and a C-terminal binding site (CBS) region consisting of amino acids  $\beta_1$ 379-408 (Zhou et al., 2001). In addition, Shiga and co-workers hypothesized that

a putative amphipathic  $\alpha$ -helix region formed by the region  $\beta_1$ 367-395 of rat-sGC mediates  $\beta_1$ -subunit dimerization with  $\alpha_1$ -sGC (Shiga and Suzuki, 2005). In good agreement with published data, the present BiFC analysis revealed that the segments  $\beta_1$ 212-222,  $\beta_1$ 304-333,  $\beta_1$ 344-363 and  $\beta_1$ 381-400 are involved in heterodimerization with  $\alpha_1$ -sGC thus confirming the importance of the identified NBS and CBS segments, and at least partially, the involvement of the predicted amphipathic helix region in sGC subunit dimerization. Furthermore, the present study goes beyond, showing that, in addition to the NBS, CBS, and the  $\alpha$ -helix contact interfaces amino acid segments  $\beta_1$ 304-333 and  $\beta_1$ 344-363 play a critical role in sGC heterodimerization. The contribution of these amino acid segments that is partially in agreement with the very early pGC-homology-based prediction of the dimerization region was not identified by the previous coprecipitation studies probably due to methodical limitations of this approach.

Concerning the sGC  $\alpha_1$ -subunit mutagenic and coprecipitation studies revealed that mainly the central region ( $\alpha_1$ 367-467) of  $\alpha_1$ -sGC mediates the heterodimerization with the corresponding  $\beta_1$ -subunit (Shiga and Suzuki, 2005; Wagner et al., 2005). Based on the known homologies (Iyer et al., 2003) it was further hypothesized that the  $\alpha_1$ -dimerization region consists of a discontinuous binding motif as already observed for the sGC  $\beta_1$ -subunit, namely an NBS- ( $\alpha_1$ 271-312) and a CBS-like region ( $\alpha_1$ 438-467; Zhou et al., 2004). In addition, structure prediction algorithms lead to the conclusion that the sGC  $\alpha_1$ -subunit may contain an amphipathic helical binding motif ( $\alpha_1$ 421-454) as postulated for the sGC  $\beta_1$ -subunit (Cary et al., 2006; Shiga and Suzuki, 2005). Further studies by site directed mutagenesis especially of conserved Leucines within the predicted  $\alpha$ -helix revealed that indeed mainly the amphipathicity of this secondary structure seems to be crucial for sGC dimerization (Shiga and Suzuki, 2005). By using the BiFC approach we were able to validate and narrow these findings. Out of the predicted region mainly the amino acids segments  $\alpha_1$ 363-372,  $\alpha_1$ 403-422 and  $\alpha_1$ 440-459 contribute to sGC dimerization suggesting a discontinuous make-up of the  $\alpha_1/\beta_1$ -sGC contact interface. In contrast to the importance of the  $\beta_1$ NBS and in good agreement with the analysis of the dimerization region of the medaka fish  $\alpha_1$ -sGC, the BiFC approach did not detect any contribution of the putative  $\alpha_1$ NBS to sGC dimerization (Shiga and Suzuki, 2005). However, in contrast to this study our deletion mutant ( $\alpha_1$ 283-292) showed enzymatic activity. This discrepancy might be explained by the fact that Shiga and Suzuki investigated a heavily truncated deletion mutant ( $\alpha_1\Delta$ 1-312) which could lead to misfolding and, as a consequence, result in the expression of non-functional sGC.

Whereas the the  $\alpha_1$ NBS seems to have no impact on sGC dimerization our BiFC approach showed that deletions of  $\alpha_1$ 440-449 and  $\alpha_1$ 450-459 within the postulated  $\alpha_1$ CBS-like site ( $\alpha_1$ 438-467) and the predicted amphipathic  $\alpha$ -helix ( $\alpha_1$ 421-454) abolished subunit dimerization and, as a result, any enzymatic activity. This observation is in good agreement with published work thus confirming the importance of the  $\alpha_1$ CBS and, in addition, the impact of the conserved leucines within the amphipathic  $\alpha$ -helix for sGC dimerization (Shiga and Suzuki, 2005). Moreover, in addition to the above discussed CBS and amphipathic  $\alpha$ -helical region, the BiFC approach revealed that the amino acid regions  $\alpha_1$ 363-372 and  $\alpha_1$ 403-422 are critical  $\alpha_1/\beta_1$ -sGC heterodimerization.

One coprecipitation study using bovine sGC reported that the N-terminal amino acids  $\alpha_1$ 61-128 mediate heterodimerization (Wagner et al., 2005). However, this sequence is not conserved and the same study showed, in good agreement with previous data, that basal activity of further deletion mutants of the N-terminal  $\alpha_1$ -subunit is preserved (Wedel et al., 1995; Wagner et al., 2005). Furthermore, the recently reported analysis of the dimerization region of medaka fish  $\alpha_1$ -sGC showed in good agreement with a previous study of the human sGC that deletion of the  $\alpha_1$ -sGC N-terminal 280 amino acids has no consequence for the activation profile of sGC thus supporting that amino acids  $\alpha_1$ 61-128 are not involved in sGC heterodimerization (Koglin and Behrends, 2003; Shiga and Suzuki, 2005).

In conclusion, the present study identified that amino acid segments  $\alpha_1$ 363-372,  $\alpha_1$ 403-422,  $\alpha_1$ 440-459,  $\beta_1$ 212-222,  $\beta_1$ 304-333,  $\beta_1$ 344-363 and  $\beta_1$ 381-400 are involved in  $\alpha_1/\beta_1$ -sGC heterodimerization and thus supports the assumption that  $\alpha_1/\beta_1$ -sGC heterodimerization is mediated via a discontinuous binding module (Fig. 4). Moreover, our results of the characterization of amino acid segments critical for  $\alpha_1/\beta_1$ -sGC dimerization in native cells support the prediction that mainly the central regions of  $\alpha_1$ - and  $\beta_1$ -sGC containing an amphipathic  $\alpha$ -helix structure are required for the formation of a functionally active  $\alpha_1/\beta_1$ -sGC heterodimer. In addition, we could herewith demonstrate that the BiFC method in combination with a cGMP readout cell line and the recently discovered modulators of sGC activity represents a powerful tool to further elucidate the process of sGC subunit dimerization and sGC activation. However, final clarification of the contribution of single amino acids to the process of dimerization is dependent on the resolution of the crystal structure of native sGC.

### **Acknowledgements**

The authors are grateful to Dr. Tom Kerppola, University of Michigan, Ann Arbor, USA for providing the BiFC vectors. We would also like to thank Yvonne Keim and Anna Kebig for the outstanding technical assistance. Dr. Peter Manuel Schmidt is recipient of an Alexander-von-Humboldt Lynen fellowship.

## References

- Alonso-Alija, C., Heil, M., Flubacher, D., Naab, P., Stasch, J.P., Wunder, F., Dembowski, K., Perzborn, E., and E. Stahl. 2001. Novel derivatives of dicarboxylic acid having pharmaceutical properties. WO-119780-A2001.03.22.
- Becker, E.M., Wunder, F., Kast, R., Robyr, C., Hoenicka, M., Gerzer, R., Schröder, H., and J.P. Stasch. 1999. Generation and characterization of a stable soluble guanylate cyclase-overexpressing CHO cell line. *Nitric Oxide*. 3:55-66.
- Bender, A.T., and J.A. Beavo. 2006. Cyclic nucleotide phosphodiesterases: molecular regulation to clinical use. *Pharmacol. Rev.* 58:488-520.
- Cary, S.P.L., Winger, J.A., Derbyshire, E.R., and M.A. Marletta. 2006. Nitric oxide signaling: no longer simply on or off. *Trends Biochem. Sci.* 31:231-239.
- Evgenov, O.E., Pacher, P., Schmidt, P.M., Haskó, G., Schmidt, H.H.H.W., and J.P. Stasch. 2006. NO-independent stimulators and activators of soluble guanylate cyclase: discovery and therapeutic potential. *Nature Rev. Drug. Discov.* 5:755-768.
- Feil, R., and B. Kemp-Harper. 2006. cGMP signalling: from bench to bedside. *EMBO Rep.* 7:149-153.
- Gerzer, R., Hofmann, F., and G. Schultz. 1981. Purification of a soluble, sodium-nitroprusside-stimulated guanylate cyclase from bovine lung. *Eur. J. Biochem.* 116:479-486.
- Gladwin, M.T. 2006. Deconstructing endothelial dysfunction: soluble guanylyl cyclase oxidation and the NO resistance syndrome. *J. Clin. Invest.* 9:2330-2332.
- Harteneck, C., Wedel, B., Koesling, D., Malkewitz, J., Böhme, E., and G. Schultz. 1991. Expression of soluble guanylyl cyclase. Catalytic activity requires two enzyme subunits. *FEBS Lett.* 292:221-223.
- Hobbs, A.J. 2002. Soluble guanylate cyclase: an old therapeutic target re-visited. *Br. J. Pharmacol.* 136:637-640.
- Hönicka, M., Becker, E.M., Apeler, H., Sirichoke, T., Schröder, H., Gerzer, R., and J.P. Stasch. 1999. Purified soluble guanylyl cyclase expressed in a baculovirus/Sf9 system: stimulation by YC-1, nitric oxide, and carbon monoxide. *J. Mol. Med.* 77:14-23.
- Honda, A., Adams, S.R., Sawyer, C.L., Lev-Ram, V., Tsien, R.Y., and W.R. Dostmann. 2001. Spatiotemporal dynamics of guanosine 3',5'-cyclic monophosphate revealed by a genetically encoded, fluorescent indicator. *Proc. Natl. Acad. Sci. USA.* 98:2437-2442.
- Hu, C.D., Chinenov, Y., and T.K. Kerppola. 2002. Visualization of interaction among bZip and Rel family proteins in living cells using bimolecular fluorescence complementation. *Mol. Cell.* 9:789-798.

- Iyer, L.M., Anantharaman, V., and L. Aravind. 2003. Ancient conserved domains shared by animal soluble guanylyl cyclases and bacterial signaling proteins. *BMC Genomics*. 4:5.
- Kerppola T.K. 2006 a. Complementary methods for studies of protein interactions in living cells. *Nat. Methods*. 3:969-971.
- Kerppola T.K. 2006 b. Visualization of molecular interactions by fluorescence complementation. *Nat. Rev. Mol. Cell. Biol.* 7:449-456.
- Koglin, M., and S. Behrends. 2003. A functional domain of the alpha1 subunit of soluble guanylyl cyclase is necessary for activation of the enzyme by nitric oxide and YC-1 but is not involved in heme binding. *J. Biol. Chem.* 278:12590-12597.
- Mergia, E., Russwurm, M., Zoidl, G. and D. Koesling. 2003. Major occurrence of the new alpha2beta1 isoform of NO-sensitive guanylyl cyclase in brain. *Cell. Signal.* 15:189-195.
- Luttrell, L.M. 2006. Transmembrane signaling by G-protein-coupled receptors. *Methods Mol. Biol.* 332:3-49.
- Nighorn, A., Byrnes, K.A., and D.B. Morton. 1999. Identification and characterization of a novel beta subunit of soluble guanylate cyclase that is active in the absence of a second subunit and is relatively insensitive to nitric oxide. *J. Biol. Chem.* 274:2525-2531.
- Nikolaev, V.O., Gambaryan, S., and M.J. Lohse. 2006. Fluorescent sensors for rapid monitoring of intracellular cGMP. *Nat. Methods*. 3:23-25.
- Nioche, P., Berka, V., Vipond, J., Minton, N., Tsai, A.L., and C.S. Raman. 2004. Femtomolar sensitivity of a NO sensor from *Clostridium botulinum*. *Science*. 306:1550-1553.
- Ozalp, C., Szczesna-Skorupa, E., and B. Kemper. 2005. Bimolecular fluorescence complementation analysis of cytochrome P450 2C2, 2E1, and NADPH-cytochrome P450 reductase molecular interactions in living cells. *Drug. Metab. Dispos.* 33:1382-1390.
- Pellicena, P., Karow, D.S., Boon, E.S., Marletta, M.A., and J. Kuriyan. 2004. Crystal structure of an oxygen-binding heme domain related to soluble guanylate cyclases. *Proc. Natl. Acad. Sci. USA*. 101:12854-12859.
- Rothkegel, C., Schmidt, P.M., Stoll, F., Schroder, H., Schmidt, H.H., and J.P. Stasch. 2006. Identification of residues crucially involved in soluble guanylate cyclase activation. *FEBS Lett.* 580:4205-4213.
- Russwurm, M., Behrends, S., Harteneck, C., and D. Koesling. 1998. Functional properties of a naturally occurring isoform of soluble guanylyl cyclase. *Biochem. J.* 335:125-130.
- Schmidt, P.M., Schramm, M., Schröder, H., Wunder, F., and J.P. Stasch. 2004. Identification of residues crucially involved in the binding of the heme moiety of soluble guanylate cyclase. *J. Biol. Chem.* 279:3025-3032.

- Schmidt, P.M., Rothkegel, C., Wunder, F., Schröder, H., and J.P. Stasch. 2005. Residues stabilizing the heme moiety of the nitric oxide sensor soluble guanylate cyclase. *Eur. J. Pharmacol.* 513:67-74.
- Shiga, T., and N. Suzuki. 2005. Amphipathic  $\alpha$ -Helix mediates the heterodimerization of soluble guanylyl cyclase. *Zoolog. Sci.* 22:735-742.
- Stasch, J.P., Becker, E.M., Alonso-Alija, C., Apeler, H., Debowsky, K., Feurer, A., Gerzer, R., Minuth, T., Perzborn, E., Pleiss, U., Schroeder, H., Schroeder, W., Stahl, E., Steinke, W., Straub, A., and M. Schramm. 2001. NO-independent regulatory site on soluble guanylate cyclase. *Nature.* 410:212-215.
- Stasch, J.P., Schmidt, P.M., Nedvetsky, P.I., Nedvetskaya, T.Y., Kumar, H.S.A, Meurer, S., Deile, M., Taye, A., Knorr, A., Lapp, H., Müller, H., Turgay, Y., Rothkegel, C., Tersteegen, A., Kemp-Harper, B., Müller-Esterl, W., and H.H.H.W. Schmidt. 2006. Targeting the heme-oxidized nitric oxide receptor for selective vasodilatation of diseased blood vessels. *J. Clin. Invest.* 116:2552-2561.
- Straub, A., Stasch, J.P., Alonso-Alija, C., Benet-Buchholz, J., Ducke, B., Feurer, A., and C. Fürstner. 2001. NO-independent stimulators of soluble guanylate cyclase. *Bioorg. Med. Chem. Lett.* 11:781-784.
- Wagner, C., Russwurm, M., Jäger, R., Friebe, A., and D. Koesling. 2005. Dimerization of nitric oxide-sensitive guanylyl cyclase requires the alpha 1 N terminus. *J. Biol. Chem.* 280:17687-17693.
- Wedel, B., Humbert, P., Harteneck, C., Foerster, J., Malkewitz, J., Böhme, E., Schultz, G., and D. Koesling. 1994. Mutation of His-105 in the beta 1 subunit yields a nitric oxide-insensitive form of soluble guanylyl cyclase. *Proc. Natl. Acad. Sci. USA.* 91:2592-2596.
- Wedel, B., Harteneck, C., Foerster, J., Friebe, A., Schultz, G., and D. Koesling. 1995. Functional domains of sGC. *J. Biol. Chem.* 278:12590-12597.
- Wilson, E.M., and M. Chinkers. 1995. Identification of sequences mediating guanylyl cyclase dimerization. *Biochemistry.* 34:4696-4701.
- Wunder, F., Stasch, J.P., Hütter, J., Alonso-Alija, C., Hüser, J., and E. Lohrmann. 2005. A cell-based cGMP assay useful for ultra-high-throughput screening and identification of modulators of the NO/cGMP pathway. *Anal. Biochem.* 339:104-112.
- Zabel, U., Weeger, M., La, M., and H.H. Schmidt. 1998. Human soluble guanylate cyclase: functional expression and revised isoenzyme family. *Biochem. J.* 335:51-57.
- Zabel, U., Häusler, C., Weeger, M., and H.H.H.W. Schmidt. 1999. Homodimerization of soluble guanylyl cyclase subunits. *J. Biol. Chem.* 274:18149-18152.

- Zhao, Y., and M.A. Marletta. 1997. Localization of the heme binding region in soluble guanylate cyclase by ODQ. *Biochemistry*. 36:15959-15964.
- Zhao, Y., Schelvis, J.P., Babcock, G.T., and M.A. Marletta. 1998. Identification of histidine 105 in the beta1 subunit of soluble guanylate cyclase as the heme proximal ligand. *Biochemistry*. 37:4502-4509.
- Zhou, Z., Gross, S., Roussos, C., Meurer, S., Müller-Esterl, W., and A. Papapetropoulos. 2004. Structural and functional characterization of the dimerization region of soluble guanylyl cyclase. *J. Biol. Chem*. 279:24935-24943.



## Figure legends

**Figure 1. Construction and validation of BiFC constructs.** (A) Fluorescence signals of YFP fragments (YN, YC) fused either at the N-terminus of sGC  $\alpha_1$ - and  $\beta_1$ -subunit ( $\alpha_1$ -YNN,  $\alpha_1$ -YCV,  $\beta_1$ -YNN,  $\beta_1$ -YCV) or at the C-Terminus of  $\alpha_1$ - or  $\beta_1$ -sGC ( $\alpha_1$ -YNH,  $\alpha_1$ -YCH,  $\beta_1$ -YNH,  $\beta_1$ -YCH). Imaging was performed by confocal microscopy of transiently transfected cGMP reporter cells. (B) Fluorescence signal of representative, transiently transfected cGMP reporter cells transfected with of  $\alpha_1/\beta_1$ -sGC, (C)  $\alpha_1$ -YCH/ $\beta_1$ -YNH-sGC and (D)  $\alpha_1$ -YNN/ $\beta_1$ -YCV-sGC. (E) Western blots of the cytosolic fractions of control and cGMP reporter cells transiently transfected with the indicated constructs. Both enzyme subunits were detected by using polyclonal antibodies as described in the Materials and methods section.

**Figure 2. Activation profile of  $\alpha_1/\beta_1$ -sGC and  $\alpha_1/\beta_1$ -sGC-YFP fusion proteins.** Activation pattern of WT-sGC (A,B),  $\alpha_1$ -YCH/ $\beta_1$ -YNH-sGC (C,D), and  $\alpha_1$ -YNN/ $\beta_1$ -YCV-sGC (E,F) incubated with increasing concentrations of BAY 41-2272 or BAY 58-2667 alone or in the presence of a fixed concentration DEA/NO (10 nM) or ODQ (10  $\mu$ M), respectively. cGMP reporter cells were transiently cotransfected with the indicated  $\alpha_1$ - and  $\beta_1$ -subunit of sGC. Enzyme activation is represented as x-fold compared with the transfected but not stimulated control. Data are shown as mean  $\pm$  S.E.M. from 3-5 independent experiments performed in quadruplicate.

**Figure 3. Activation of  $\alpha_1/\beta_1$ -sGC and  $\alpha_1/\beta_1$ -sGC-YFP fusion proteins by DEA/NO.** Activation of WT-sGC (white bar),  $\alpha_1$ -YCH/ $\beta_1$ -YNH-sGC (grey bar), and  $\alpha_1$ -YNN/ $\beta_1$ -YCV-sGC (black bar) alone or incubated with DEA/NO (10 nM). cGMP reporter cells were transiently cotransfected with the indicated  $\alpha_1$ - and  $\beta_1$ -subunit of sGC. Enzyme activation is represented as x-fold compared with the transfected but not stimulated control. Data are shown as mean  $\pm$  S.E.M. from 3-5 independent experiments performed in quadruplicate.

**Figure 4. Overview of identified dimerization regions of  $\alpha_1/\beta_1$ -sGC.** Multisequence alignment of sGC  $\alpha$  and  $\beta$  subunits from the following species (accession numbers in brackets): rat  $\alpha_1$  (P19686), bovine  $\alpha_1$  (P19687), human  $\alpha_1$  (Q02108), mouse  $\alpha_1$  (Q9ERL9), Medaka fish  $\alpha_1$  (P79997), rat  $\beta_1$  (P20595), bovine  $\beta_1$  (P16068), human  $\beta_1$  (Q02153), mouse  $\beta_1$  (O54865), medaka fish  $\beta_1$  (P79998), drosophila  $\beta_1$  (Q24086). Conserved residues are colored in red. The start- / endpoint of the H-NOX and catalytic domains, respectively, is shaded in blue. sGC  $\alpha_1/\beta_1$  interaction sites reported in the present work or by others are highlighted as follows: Amino acid

regions contributing to  $\alpha_1/\beta_1$ -sGC dimerization are marked in orange. Segments that are not involved in subunit dimerization but seem to be critical for functional enzyme activity are highlighted in yellow. Regions analyzed and identified to be neither involved in  $\alpha_1/\beta_1$ -sGC dimerization nor critical for sGC activity are shaded in green. The conserved leucines mentioned in the text are highlighted in blue.

**Figure 5. Fluorescence and expression signals of sGC deletion mutants.** (A) Fluorescence signal of representative cGMP reporter cells transiently transfected and imaged by confocal microscopy. (B) Western blots of the cytosolic fractions of cGMP reporter cells transiently transfected with the indicated deletion mutants and Actin which were detected as described in the Materials and Methods section.

**Figure 6. Activation profile of sGC deletion mutants.** Activation pattern of the indicated YFP-sGC constructs incubated with increasing concentrations of BAY 41-2272 or BAY 58-2667 alone or in the presence of a fixed concentration DEA/NO (10 nM) or ODQ (10  $\mu$ M), respectively. cGMP reporter cells were transiently cotransfected with the  $\alpha_1$ - and  $\beta_1$ -subunit of sGC. Enzyme activation is represented as x-fold compared with the transfected but not stimulated control. Data are shown as mean  $\pm$  S.E.M. from 3-5 independent experiments performed in quadruplicate.

**Table I. Primers used to introduce BsiWI and ClaI restriction sites in pcDNA/Amp- $\alpha_1$ , pRNAI/Amp- $\beta_1$ , pBiFC-YN154, and pBiFC-YC155 to generate YFP-sGC fusion proteins**

Plasmid	Vector	Primer
<b>YCV</b>	pHA/CMV (Clonotech)	
BsiWI site		5'-GCCATGGAGGCCGTACGTCGGGTCGTG-3'
ClaI Site		5'-GTCGGGGTCGTGATCGATCCATCGGTCGTC-3'
<b>YCH</b>	pHA/CMV (Clonotech)	
BsiWI site		5'-GCTGTACAAGTACGTACGCGCGGGGATCC-3'
ClaI Site		5'-GACATGATAAGATCGATTGATGAGTTTGGAC-3'
<b>YNV</b>	pFlag/CMV-2 (Sigma)	
BsiWI site		5'-CTTGTCCCCCATCGTACGGGAGTCTCAGGAG-3'
ClaI Site		5'-GCATGAGAAATCGATTCGCTGCCTC-3'
<b>YNH</b>	pFlag/CMV-2 (Sigma)	
BsiWI site		5'-CTATATCATGGCCGTACGATCCCGGGTGGC-3'
ClaI Site		5'-GTGACCCCTCCCAATCGATCTCCTGGC-3'
<b><math>\alpha_1</math>-sGC</b>	pcDNAI/Amp (Invitrogen)	
BsiWI site		5'-CCACTGCAAAGCGTACGGAACACCATG-3'
Cla Site		5'-CATCAGGGGTAGATCGATGAGCCGCATG-3'
<b><math>\beta_1</math>-sGC</b>	pRNAI (Invitrogen)	
BsiWI site		5'-CAGGCTCCGGGCGTACGGTACACCATG-3'
Cla Site		5'-CAGGATGAAAATCGATTGGCAGCC-3'

**Table II. Primers used to generate deletion mutants within the proposed dimerization domains of both sGC subunits as described in the materials and methods section**

Mutation	Primer
$\alpha_1$ ( $\Delta$ 283 – 292) -YNV	5'-CTAGTGATCCCTACTTCGCTCCTGGACCGTGACCTGGCCATTG-3'
$\alpha_1$ ( $\Delta$ 363 – 372) -YNV	5'-GTGAAGAAATCTTCAAGGGTTGTTGAATCCAGTGCCATCTTGTTG-3'
$\alpha_1$ ( $\Delta$ 373 – 382) -YNV	5'-TCAAAGGTCAAATGATCTACATCTCGCCGTGTGTGGACAGATTGG-3'
$\alpha_1$ ( $\Delta$ 383 – 392) -YNV	5'-GTGCCATCTTGTTCTTAGGGACAGGACGGGGTCTCTATCTG-3'
$\alpha_1$ ( $\Delta$ 393 – 402) -YNV	5'-GTGGACAGATTGGAAGATTTCCCGATTGATAATGCCCTGAGG-3'
$\alpha_1$ ( $\Delta$ 403 – 412) -YNV	5'-CGGGGTCTCTATCTGTCTGACATCTTGATAGGGGAACAGGCACGG-3'
$\alpha_1$ ( $\Delta$ 413 – 422) -YNV	5'-CATAATGCCCTGAGGGATGTTGTCTGGCCTCAAGAAGAGGTTGGG-3'
$\alpha_1$ ( $\Delta$ 440 – 449) -YNV	5'-CCTTGGAGCATGCCCACCAAGTAGATCTCCTGTGTTCTATC-3'
$\alpha_1$ ( $\Delta$ 450 – 459) -YNV	5'-GAGGAGGAGAAGAAGAAGACGGAGGTTGCTCAGCAGCTCTGGC-3'
$\alpha_1$ ( $\Delta$ 460 – 469) -YNV	5'-CTGTGTTCTATCTTTCCCTCTATTGTGCAAGCCAAGAAGTTC-3'
$\alpha_1$ ( $\Delta$ 470 – 479) -YNV	5'-CAGCAGCTCTGGCAAGGACAAACCATGCTCTTCTCAGATATC-3'
$\beta_1$ ( $\Delta$ 212 – 222) -YCV	5'-GACTCCCGTATCAGCCCGTACATATTTGACCGGGACCTAGTAG-3'
$\beta_1$ ( $\Delta$ 304 – 313) -YCV	5'-CTGGGGCAGAGATTAGCTGCCCGGAAGCAGATAGCATCCTC-3'
$\beta_1$ ( $\Delta$ 314 – 323) -YCV	5'-CAAAGGCCAAATGATCTATTTATCACCAGTGTGATGAACCTG-3'
$\beta_1$ ( $\Delta$ 324 – 333) -YCV	5'-GATAGCATCCTCTTCTCTGTACAAGAAGAGGCCTGTACCTG-3'
$\beta_1$ ( $\Delta$ 334 – 343) -YCV	5'-GTGATGAACCTGGATGACCTACCTCTCCATGATGCTACACGAG-3'
$\beta_1$ ( $\Delta$ 344 – 353) -YCV	5'-GAGGCCTGTACCTGAGTGACATCCTTTTGGGAGAACAGTTCCGG-3'
$\beta_1$ ( $\Delta$ 354 – 363) -YCV	5'-GATGCTACACGAGACCTGGTCAACTGACACAAGAGCTGGAAATC-3'
$\beta_1$ ( $\Delta$ 381 – 390) -YCV	5'-CAGGCTGCAGCTCACACTGGACACATTGCTATATTCTGTTG-3'
$\beta_1$ ( $\Delta$ 391 – 400) -YCV	5'-GAGGATGAGAAGAAAAAGACATCTGTTGCCAATGAGCTGAGAC-3'
$\beta_1$ ( $\Delta$ 401 – 410) -YCV	5'-CTATATTCTGTTCTCCCTCCACAGTGCCGGCCAAAAGATAC-3'
$\beta_1$ ( $\Delta$ 411 – 420) -YCV	5'-CAATGAGCTGAGACACAAGCGTACCATCCTCTTCAGTGGCATTGTG-3'

# Figure 1

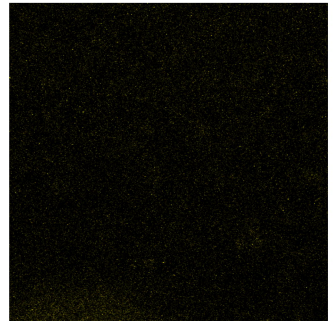
**A**

## Fluorescence signal

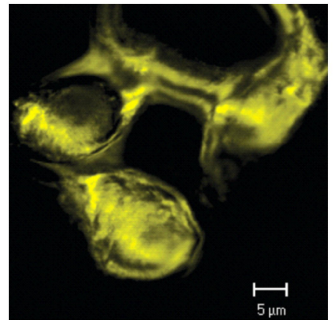
Untransfected control	n.d. <sup>a</sup>
$\alpha_1/\beta_1$ -sGC	n.d.
$\alpha_1$ -YCV/ $\beta_1$ -YNV-sGC	n.d.
$\alpha_1$ -YCH/ $\beta_1$ -YNH-sGC	+
$\alpha_1$ -YNV/ $\beta_1$ -YCV-sGC	+
$\alpha_1$ -YNH/ $\beta_1$ -YCH-sGC	n.d.
$\alpha_1$ -YCV/ $\beta_1$ -YNH-sGC	n.d.
$\alpha_1$ -YCH/ $\beta_1$ -YNV-sGC	n.d.
$\alpha_1$ -YNV/ $\beta_1$ -YCH-sGC	n.d.
$\alpha_1$ -YNH/ $\beta_1$ -YCV-sGC	n.d.
$\alpha_1$ -YCH/ $\alpha_1$ -YNV-sGC	n.d.
$\alpha_1$ -YCH/ $\alpha_1$ -YNH-sGC	n.d.
$\alpha_1$ -YNV/ $\alpha_1$ -YCV-sGC	n.d.
$\alpha_1$ -YNV/ $\alpha_1$ -YCH-sGC	n.d.
$\beta_1$ -YCV/ $\beta_1$ -YNV-sGC	n.d.
$\beta_1$ -YCV/ $\beta_1$ -YNH-sGC	n.d.
$\beta_1$ -YNH/ $\beta_1$ -YCV-sGC	n.d.
$\beta_1$ -YNH/ $\beta_1$ -YCH-sGC	n.d.

<sup>a</sup>n.d., not detectable

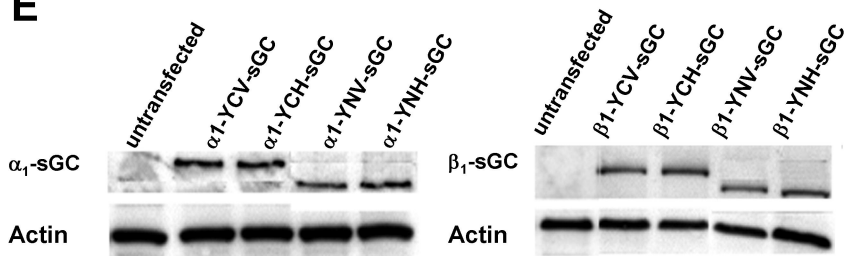
**B**



**C**



**E**



**D**

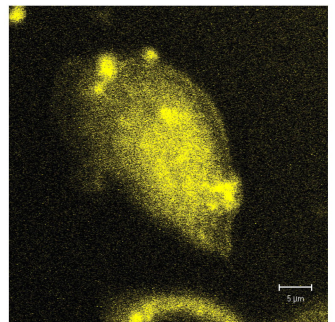


# Figure 2

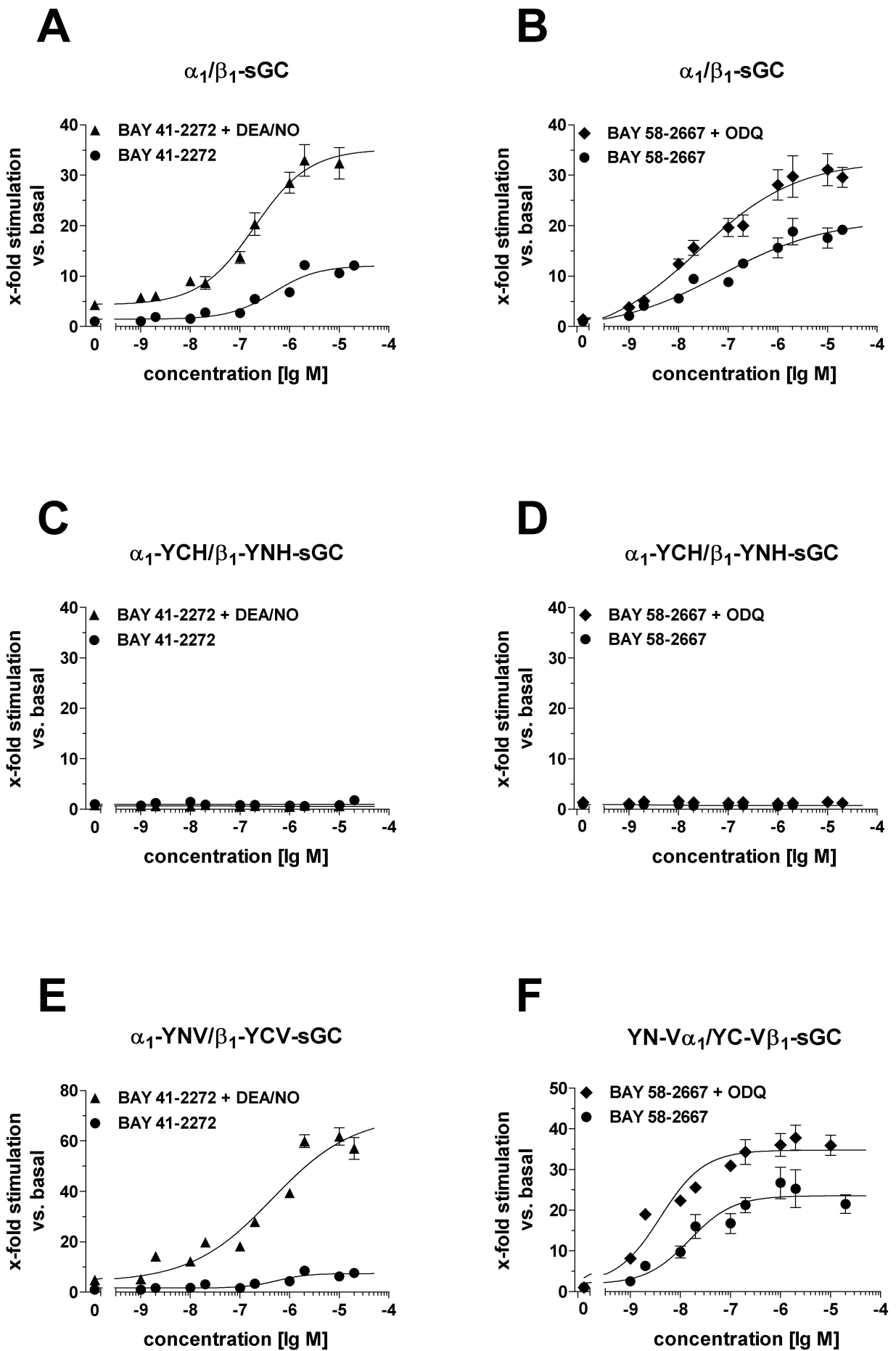


# Figure 3

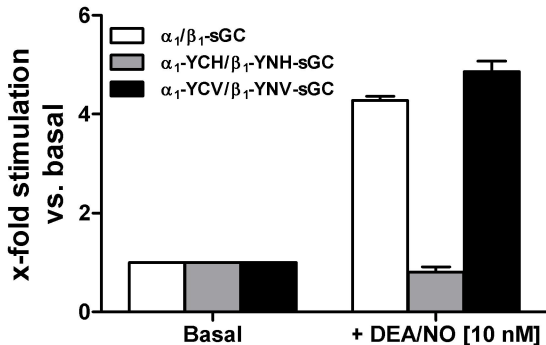


# Figure 4

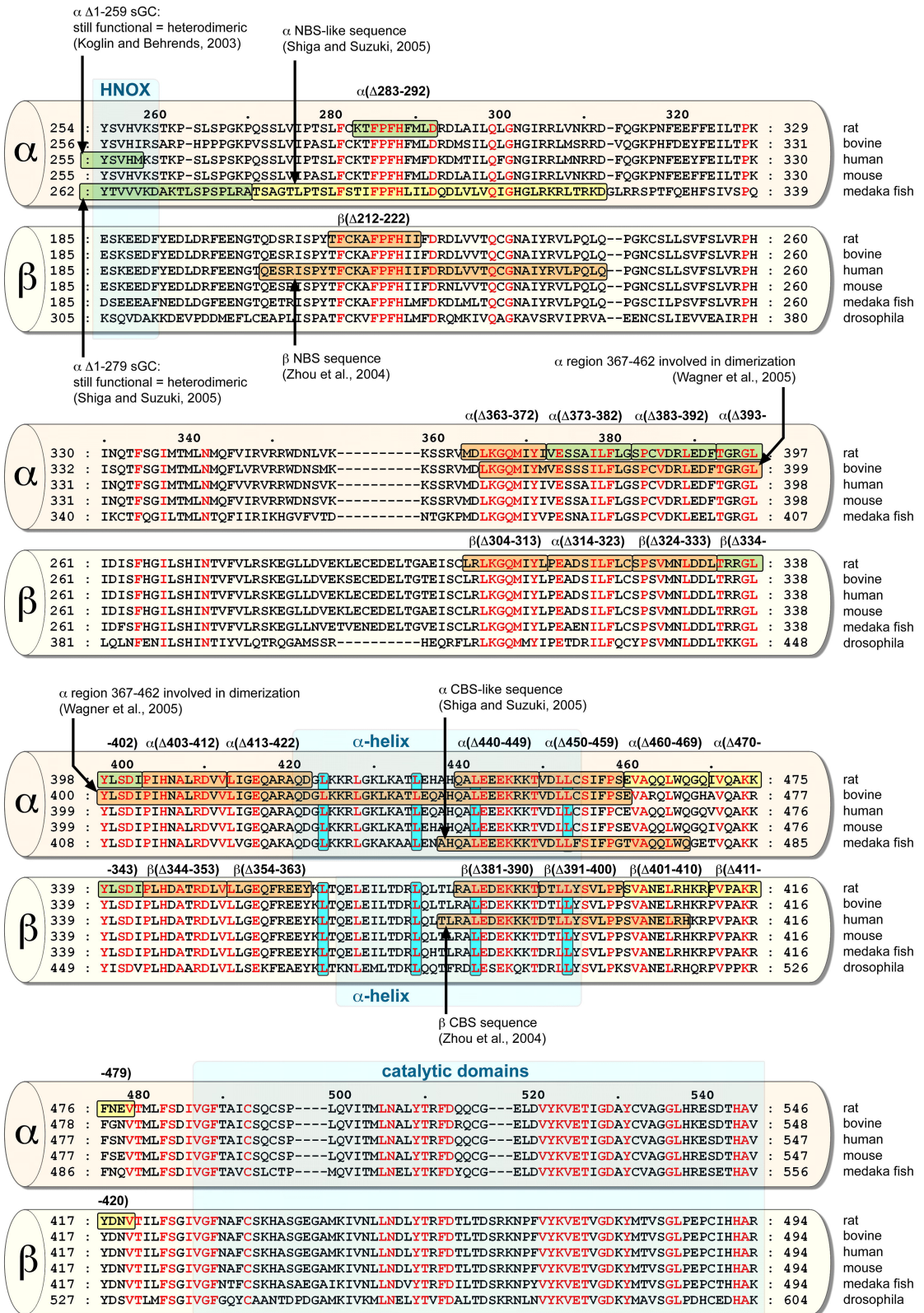
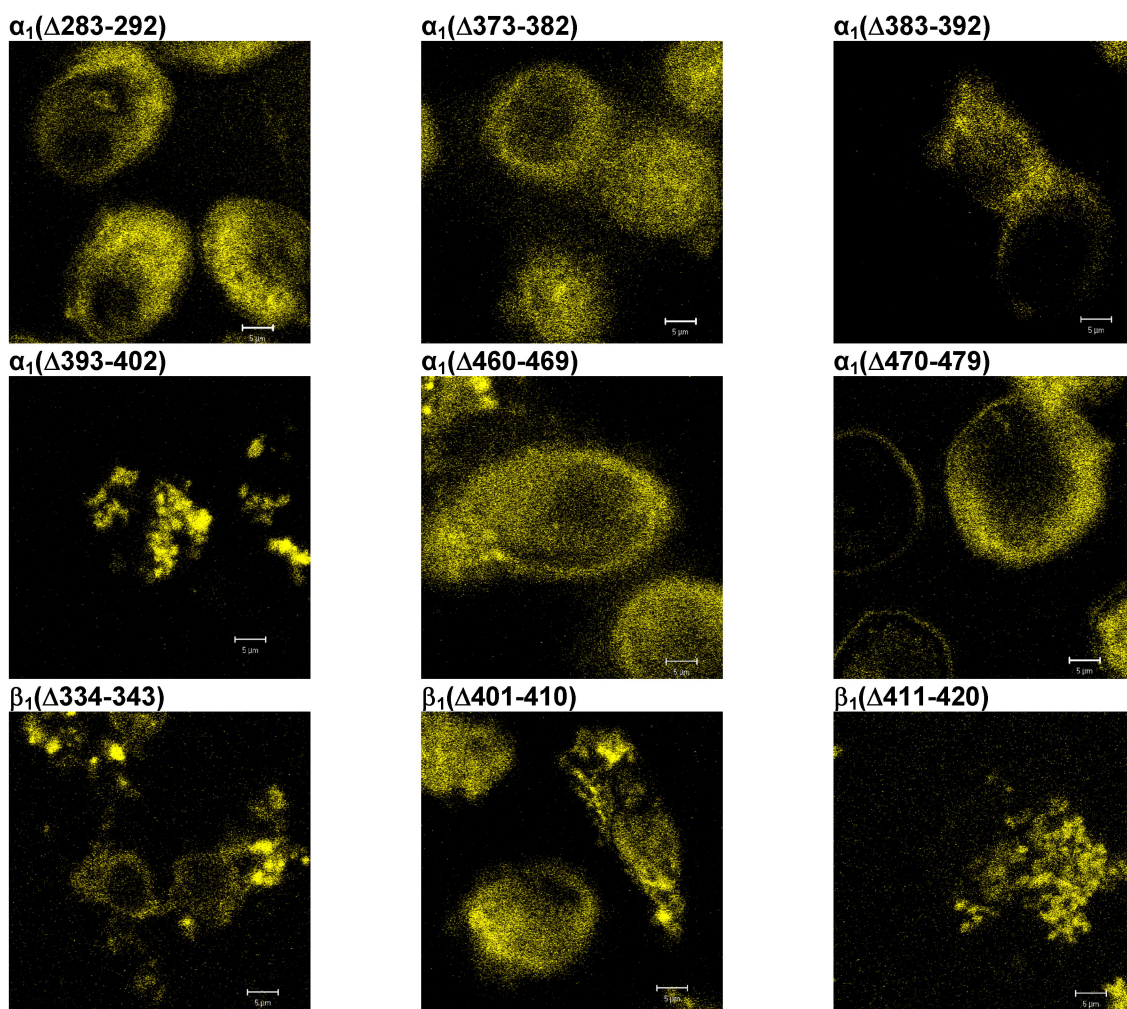


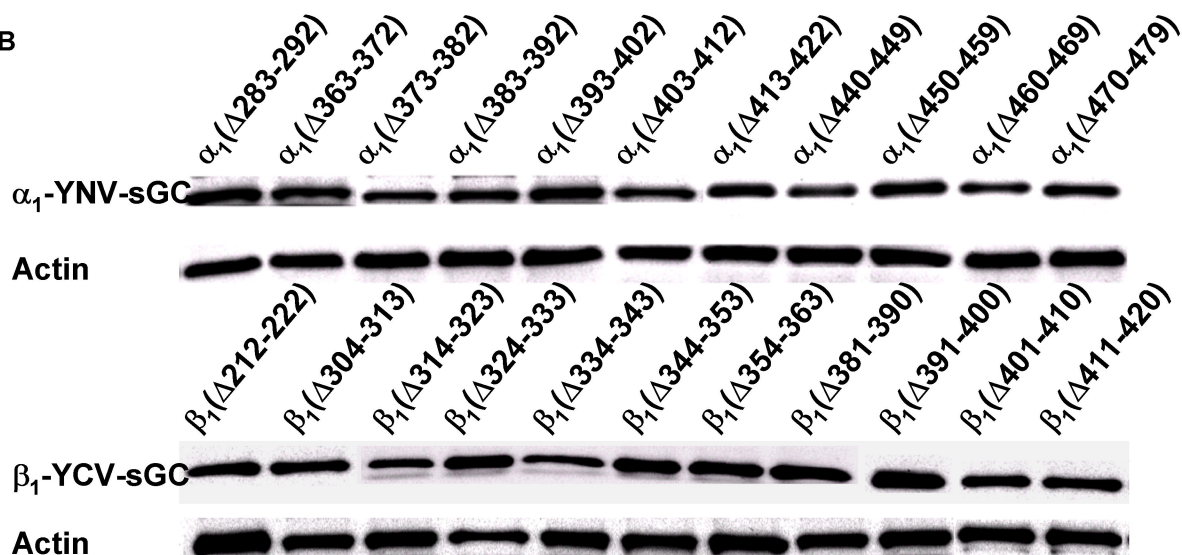


Figure 5

A



B



# Figure 6

